This Article is under Formatting, the PDF's ready file will be replaced soon.

Journal of Catalyst & Catalysis
E-ISSN:2349-4344
Volume- 13 Issue- 01 Year- 2026
Review Article
Received Date: April 18, 2026
Accepted Date: April 20, 2026
Published Date: April 30, 2026

Advances in Photocatalytic Catalysts for Wastewater Treatment

[1]Rakshit Ameta, [2]Lalita Joshi, [3]Deepika Patel, [4]Jyotsana Panwar, [5]Suresh C. Ameta, [6]R.M.Aadarsh Vel, [7]R.Madhumitha Sri, [*8]S.Ravichandran

[1-5]Department of Chemistry, PACIFIC University, Udaipur, Rajasthan.

[6]BBA Student in Airlines & Airport Management, Lovely Professional University, Jalandhar, Punjab.
[7]B.Tech. Student in Anna University & Validation Analyst (R&D), Zifo Technology, Chennai.
[8]Professor in Chemistry, St.Peter's Institute of Higher Education and Research, Chennai.
Corresponding mail **:**drravichandran.chemistry@spiher.ac.in

Abstract:

Water is a fundamental component of the life support system and is indispensable for the survival of all living organisms. Life cannot exist without water, and human societies depend on it for drinking, agriculture, industry, and sanitation. Water resources are increasingly under pressure in terms of both quality and availability, largely due to rapid industrial development, expanding urban areas, and rising population levels. These human-driven activities have played a major role in polluting both surface water and groundwater systems.

Key contributors to water pollution include industrial wastewater, agricultural runoff, domestic sewage, and other forms of waste. Effluents from industries often carry toxic chemicals, heavy metals, and hazardous materials that deteriorate water quality. In a similar manner, agricultural practices lead to the introduction of pesticides, fertilizers, and other harmful substances into nearby water bodies through surface runoff. Additionally, untreated or inadequately treated sewage worsens the situation by adding disease-causing microorganisms and organic contaminants. Consequently, such pollution renders water unfit for drinking, irrigation, and other vital applications.

On a global scale, water pollution is strongly associated with insufficient sanitation facilities. It is estimated that over 2.6 billion people—nearly 40% of the global population—still do not have

access to basic sanitation. This deficiency in sanitation infrastructure significantly contributes to the ongoing contamination of water resources. Consequently, over 10% of the global population relies on drinking water that is unsafe and poses serious health risks.
Addressing water pollution requires sustainable management practices, improved wastewater treatment, and increased awareness to ensure safe and clean water for present and future generations.
Keywords: Water pollution, Industrial effluents, Urbanization, Agricultural runoff, Sewage contamination, Anthropogenic activities, Water quality, Sanitation, Drinking water safety.

Memory full
Responses may feel less personalized. Upgrade to expand memory, or manage existing memories.

1.1 Introduction:

Water is an essential natural resource for human survival. However, contamination of water sources has become a significant challenge for humanity. Microbial and chemical contamination challenges are there before the world in providing safe and clean water to the society. Organic pollutants in industrial and agricultural sewage are a serious threat to the environments as well as human health. Major water pollutants are represented in Figure 1.

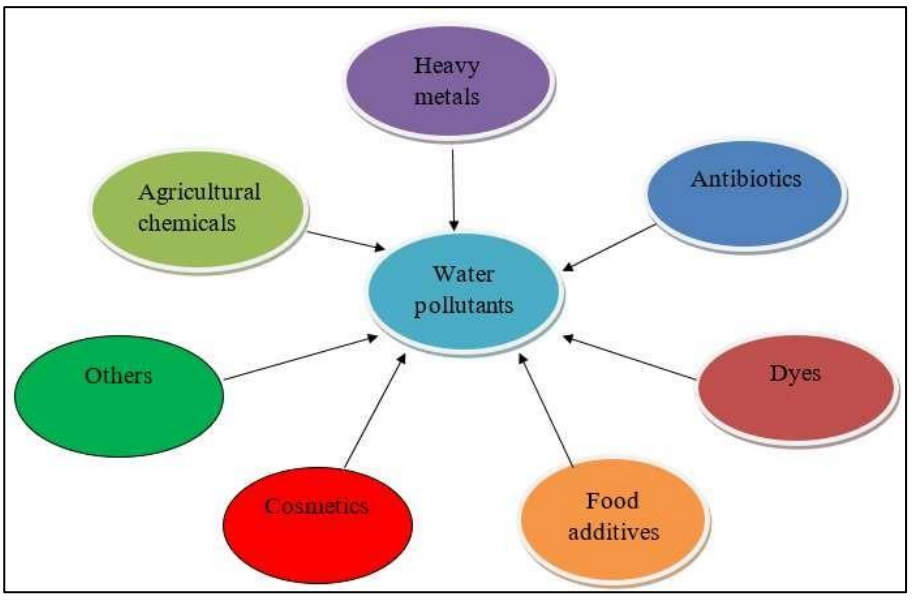

Figure 1.1: Major Water Pollutants

They contribute significantly to water pollution. As a result, thousands of children lose their lives each day due to various waterborne diseases, including diarrhea, cholera, and typhoid. The adverse effects of water pollution still remained a major source of causing health problems. These are represented in Figure 2.

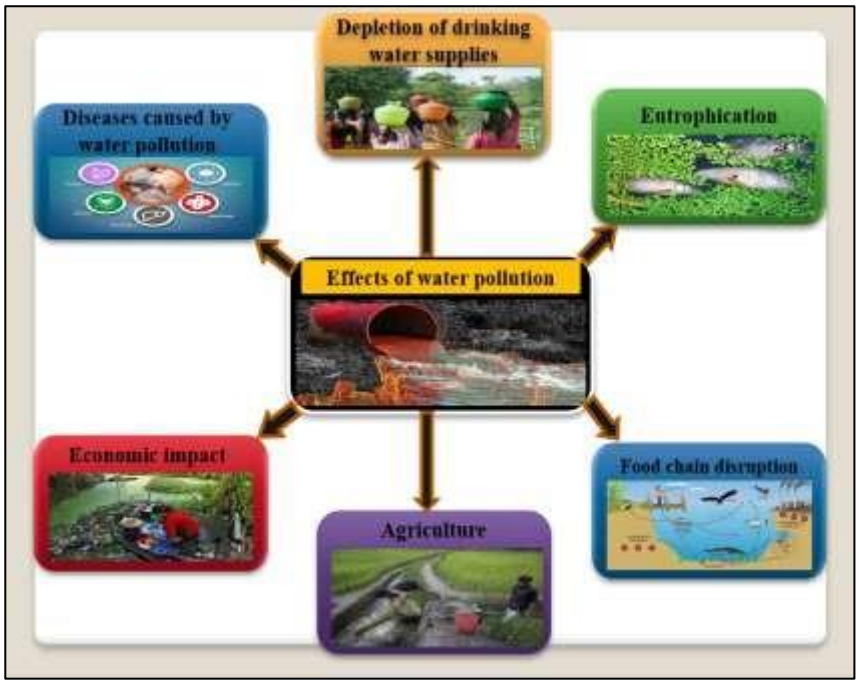

Figure 2: Adverse Effects of Water Pollution

Literature Review

Some of these known techniques used for water and wastewater treatment are:

- Electrodeposition,
- Electrocoagulation,
- Electro flotation,
- Electrooxidation,
- Screening, aeration and pre-chlorination,
- Filtration,
- Settling or sedimentation,
- Coagulation and flocculation,
- Disinfection and chlorination,
- Aeration,
- Biofiltration, and
- Oxidation ponds.

Various wastewater treatment technologies are available, which are different from each other is regards to their principles, economy, application, and speed. Common methods of wastewater treatment are classified as biological, chemical and physical treatments.

Many methods of treatment of pollution water have been suggested and used for last few decades. But all these methods are associated with some or the other disadvantage. Therefore, there is a need for fast, low cost, effective and green chemical technology and search is still on. Advanced oxidation process (AOPs) are significantly efficient for complete destruction of pollutants like, naturally occurring toxins, pesticides,

dyes, phenols, EDS, etc. AOPs have been proposed to degrade even recalcitrant molecules. Advanced oxidation process is a wastewater treatment process, which is used to convert polluted water into useful form with relatively less or negligible health and environment issues. Treated waste water is then returned back to water-cycle and it can be reused.

1.2 Advanced Oxidation Processes (AOPs):

Advanced oxidation processes (AOPs), in a broad sense, encompass a range of chemical treatment methods aimed at eliminating organic—and in some cases inorganic—contaminants from water and wastewater. These processes rely on oxidation reactions involving highly reactive species such as hydroxyl radicals (•OH), positive holes (h^+), superoxide anion radicals ($O_2•^-$), and hydroperoxyl radicals ($HO_2•$), among others. The principal categories of AOPs include photolysis, photocatalysis, electrochemical oxidation, sonolysis, Fenton-based reactions, and ozone-based processes.

- **Advanced oxidation processes (AOPs) offer multiple benefits in water treatment applications:**
-
- **• They are capable of efficiently degrading organic contaminants directly in the aqueous phase, avoiding the need to transfer pollutants into another medium.**
-
- **• Owing to the highly reactive nature of hydroxyl radicals (•OH), these processes can non-selectively react with a wide range of dissolved pollutants. This makes AOPs particularly suitable for treating water containing multiple organic contaminants simultaneously.**
-
- **• Certain heavy metals can also be eliminated through the formation and precipitation of metal hydroxides, represented as $M(OH)_x$.**
-
- **• In some cases, AOPs also provide disinfection, enabling them to function as a combined solution for both contaminant removal and microbial control.**
-
- **• Since the ultimate by-product of hydroxyl radical reactions is water, AOPs theoretically do not introduce additional hazardous substances into the treated water.**

One of the major advantages of AOPs is transformation or complete mineralization of organic pollutants; even persistent organic pollutants (POPs) to simple stable inorganic compounds such as water, carbon dioxide, and salts with negligible or no sludge production. Hence, it may not require another sludge treatment stage.

1.3 Photocatalysis:

Photocatalysis is a developing branch of chemistry, which deals with chemical reactions proceeding in the presence of light and photocatalyst. Basically, a photocatalyst is a semiconductor, which increases the rate of a reaction in presence of light. There is a wide

range of applications of photocatalyst such as water purification, antibacterial, deodorizing, air purifying, antifogging, self-cleaning, etc.

Here, superhydrophilicity played an important role. As it is a green chemical route and therefore, it is the requirement of the day. A photocatalyst is derived from two terms: "photo," referring to light or photons, and "catalyst," which denotes a substance that modifies the rate of a chemical reaction without being consumed. Thus, photocatalysts are materials that influence reaction rates when exposed to light, a process termed photocatalysis. In this context, a photocatalyst is a substance that absorbs light and facilitates chemical transformations. Most photocatalysts are semiconducting materials. Photocatalysis involves the generation of electron–hole pairs when a semiconductor is irradiated with light. The excited electrons in the conduction band participate in reduction reactions, while the holes in the valence band lead to the formation of highly reactive hydroxyl radicals (•OH), which are strong oxidizing agents capable of degrading various organic compounds. The overall photocatalytic mechanism is illustrated in Figure 3.

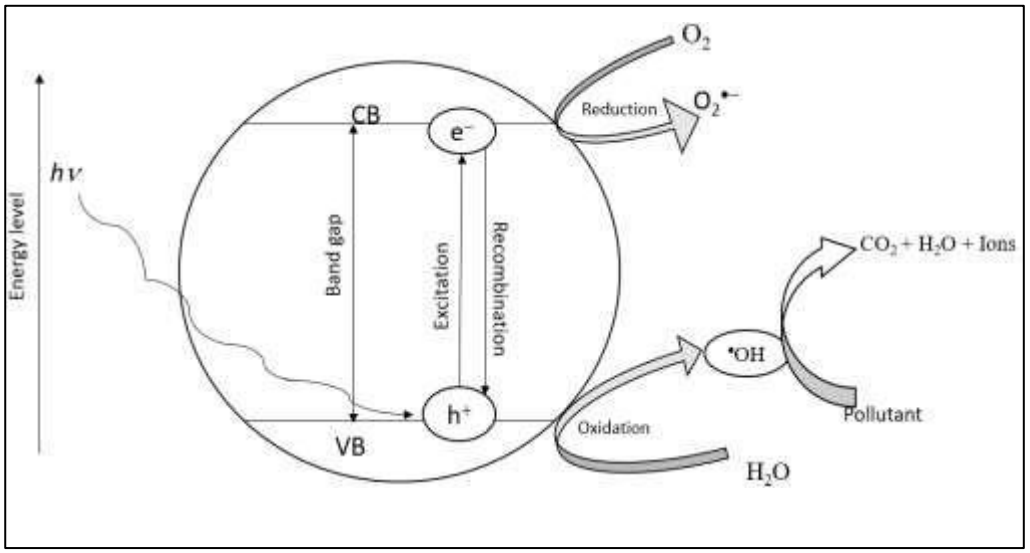

Figure 3: Mechanism of Photocatalysis

Photocatalytic processes are broadly divided into two categories based on the physical states of the reactants involved:

• Homogeneous photocatalysis: This occurs when the semiconductor and the reactant exist in the same phase—whether gas, liquid, or solid.
• Heterogeneous photocatalysis: This type takes place when the semiconductor and the reactant are present in different phases.

Photocatalysts are materials capable of breaking down harmful substances when exposed to sunlight, particularly ultraviolet radiation. Among the commonly used photocatalysts, titanium dioxide (TiO_2) and zinc oxide (ZnO) have been extensively studied. Of the various crystalline forms of TiO_2, the anatase phase exhibits superior photocatalytic activity. Photocatalysts can be synthesized using several techniques, including sol–gel, co-precipitation, hydrothermal, solvothermal, sonochemical, and chemical

vapor deposition methods. These materials find wide-ranging applications such as antifouling, antifogging, energy conservation and storage, deodorization, sterilization, self-cleaning surfaces, air purification, and wastewater treatment.

Modification of Photocatalyst

Efficiency of a photocatalyst can be enhanced by:

- Formation of localized state just above the valence band,
- Formation of localized state just below the conduction band,
- Using photocatalyst with low band gap, and
- Color center formation in band gap and surface modification.

Some of the important techniques for modification of photocatalyst are:

- Doping with metal or nonmetal,
- Codoping with various combination of donor and acceptor materials,
- Coupling of photocatalyst, composite formation,
- Sensitization,
- Use of co-catalyst, and
- Use of heterojunction (Z-scheme and S- scheme).

1.4 Photocatalytic Degradations:

Photocatalytic degradation is an advanced oxidation technique employed to break down pollutants that are present at high concentrations, exhibit structural complexity, and resist biodegradation. This process utilizes light energy to initiate and accelerate the decomposition of contaminants.

In a study conducted by Ledakowicz et al., synthetic wastewater and model effluents from the knitting industry were treated using advanced oxidation processes (AOPs). The wastewater composition included an anionic detergent (Awiważ KG), a softening agent (Tetrapol CLB), and Acid Blue 40 (AB40). The findings indicated that AB40 could not be biodegraded in the absence of AOP pre-treatment.

Furthermore, the researchers examined the influence of different oxidizing agents, such as hydrogen peroxide (H_2O_2) and ozone (O_3), under ultraviolet (UV) irradiation, on enhancing the biodegradability of textile wastewater. Tang et al.[2] investigated photocatalytic degradation of methylene blue (MB) over $CaIn_2O_4$ photocatalyst under visible light irradiation in 2 h at room temperature. It was reported that high activity could be retained in a wide range of wavelength even up to 580 nm. The SO^{2-} ions were detected as a product of degradation of MB, indicating that this dye was completely mineralized in this process.

Liqiang et al.[3] modified ZnO nanoparticles photocatalysts by depositing Pd on their surfaces via photoreduction method. It was observed that content of crystal lattice oxygen decreased on surface of ZnO nanoparticles, when sufficient amount of Pd was deposited, but adsorbed oxygen increased, which indicated that Pd was deposited on the crystal lattice oxygen. As a result, the activity of ZnO nanoparticles was significantly improved in gas phase photocatalytic oxidation of *n*-C_7H_{16}. It was concluded that photocatalytic activity of Pd-deposited ZnO nanoparticles was higher.

Chen et al.[4] prepared a visible light active TiO_2 photocatalyst via surface chemical modification using toluene 2,4-diisocyanate (TDI). It was reported that as-prepared TiO_2-TDI had absorption in the visible region due to LMCT excition of the surface complex. This TiO_2-TDI photocatalyst had a good photostability and it also exhibited high photocatalytic performance for the degradation of organic pollutants. It was revealed that turnover number of this photocatalyst for photodegradation of 2,4-dichlorophenol could reach 15.43 after five times reuse of this photocatalyst under visible light irradiation.

Wu et al.[5] prepared boron and carbon modified visible light-active TiO_2 photocatalyst through sol–gel followed by a solvothermal process. It was reported that as-prepared boron and carbon modified TiO_2 exhibited absorption in visible range (400–500 nm). It was also revealed that there is oxygen vacancy also in samples of carbon and boron modified TiO_2. It was found that this modified TiO_2 has higher photocatalytic activity on the degradation of acid orange 7 (AO7) in aqueous solution on visible light exposure than carbon modified TiO_2 and undoped anatase TiO_2.

Pan and Zhu[6] synthesized $BiPO_4$ with a nonmetal oxy acid via hydrothermal method. The as-prepared $BiPO_4$ photocatalyst has a band gap of 3.85 eV. It was found that the photocatalytic activity of $BiPO_4$ was almost double than that of TiO_2 (P25, Degussa) in degradation of methylene blue (MB), but BET surface area of $BiPO_4$ is just one tenth of compared to TiO_2 P25.

It was revealed that higher position of the valence band and separation efficiency of electron−hole pairs are responsible for higher photocatalytic activity of $BiPO_4$. It was concluded that an inductive effect of PO_4^{3-} helped in separation of e^-/h^+ providing $BiPO_4$ an excellent photocatalytic activity.

Yu et al.[7] prepared Fe (III)/AgBr photocatalysts by grafting Fe (III) cocatalyst on surface of AgBr particles via an impregnation method. They evaluated photocatalytic performance by the photocatalytic decolorization of methyl orange solution in presence of visible-light. It was reported that the Fe (III) cluster acted as an effective cocatalyst. It not only improved the photocatalytic activity of AgBr photocatalyst, but it also increased photoinduced stability of photosensitive AgBr. It was revealed that photocatalytic activity of AgBr photocatalyst surface coated by Fe (III) cocatalyst (8.2 at. %) was enhanced by a factor of 73% and it can be reused even after five cycles.

Bai et al.[8] A C_{60}-modified graphitic carbon nitride composite (C_{60}/g-C_3N_4) was synthesized through thermal treatment at 550 °C, involving the polymerization of dicyandiamide in the presence of C_{60}. It was reported that the valence band (VB) of g-C_3N_4 shifted to a lower energy state, when C_{60} was incorporated into the matrix of g-C_3N_4. It provides strong photo-oxidation capability to as-prepared composite under visible light. This composite exhibited enhanced degradation of methylene blue (MB) and phenol in presence of visible light ($\lambda > 420$ nm). The C_{60}/g-C_3N_4 composites had high photocatalytic degradation activities as compared to bulk g-C_3N_4. This enhanced photocatalytic activity may be due to holes and $^{\bullet}OH$ radicals. It may be attributed to strong interaction of conjugative π-bond between g-C_3N_4 and C_{60}.

The ZnO nanoneedles (ZNNs) were grown by Tripathy et al.[9] in large quantity by thermal evaporation approach on non-catalytic silicon substrates. It was then used as effective photocatalyst for photocatalytic degradation of methyl orange (MO). It was observed that

as-synthesized nanostructures were having high density and exhibited high-crystallinity with good optical properties. The photocatalytic properties of ZNNs were investigated under UV light irradiation. It was also revealed that degradation rate of ~95.4% of MO could be achieved within 140 min. Balcha et al.[10] Zinc oxide nanoparticles were synthesized using both precipitation and sol–gel techniques. Structural analysis confirmed the formation of a hexagonal wurtzite phase, with crystallite sizes of approximately 30 nm and 28 nm for the precipitation and sol–gel methods, respectively. The photocatalytic performance of the prepared materials was assessed through the degradation of methylene blue under UV irradiation. Results indicated that for dye concentrations ranging from 20 to 100 mg L^{-1}, degradation efficiencies of 81.0% and 92.5% were achieved using ZnO (250 mg L^{-1}) synthesized via precipitation and sol–gel routes, respectively. These findings suggest that the sol–gel method is more effective and preferable compared to the precipitation approach.
Thi and Lee[11] prepared visible light-driven photocatalysts of lanthanum (La) doped ZnO nanoparticles via precipitation method using different La doping concentrations (0.5, 1.0 and 1.5 wt%). It was reported that although La doping did not affect the crystallinity of ZnO much more, but it increased optical absorption of visible light due to the reduction in band gap energy and particle size. The La-doped ZnO photocatalyst was then used for treatment of paracetamol (100 mg L^{-1}) in aqueous solution for 3 h under visible light irradiation. It was revealed that 1.0 wt% La-doped ZnO photocatalyst exhibited highest photocatalytic activity in degrading paracetamol and it could achieve a degradation efficiency of 99% and TOC removal of 85%.
Sudrajat and Babel[12] synthesized N-doped ZnO (N-ZnO) via combustion route. The photocatalytic performance of N-doped ZnO (N–ZnO) was assessed for the degradation of amaranth (AM) and methylene blue under both visible and ultraviolet (UV) irradiation. It was reported that N-doping extended the spectral response in visible region and even up to the near-infrared region using 1 g L^{-1} of N-ZnO at pH 7. It was also revealed that 89.3% of methylene blue (10 mg L^{-1}) could be degraded within 1.5 h under visible light, while 4 h are required with N-ZnO and it can degrade only 88.5% of amaranth.
Wu et al.[13] constructed a composite of *p*-type $LaFeO_3$ microspheres coated with *n*-type nanosized graphitic carbon nitride nanosheets (g-C_3N_4). It was reported that as-prepared $LaFeO_3$/g-C_3N_4 *p-n* heterostructured photocatalyst exhibited enhanced visible-light absorption, efficient and effective separation and migration of charge carriers. As a result, this composite displayed higher visible-light photocatalytic activity for the degradation of brilliant blue, which was 7.8 and 16.9 times than that of $LaFeO_3$ and pristine g-C_3N_4, respectively. The photogenerated holes, superoxide radicals and hydroxyl radicals played active role as oxidants in this degradation process. Z-scheme charge carrier transfer pathway has been proposed to explain this dye-sensitization effect.

Huang et al.[14] prepared molybdenum disulfide (MoS_2) microspheres and used them as a photocatalyst for the degradation of thiobencarb (TBC) in presence of visible-light. It was reported that degradation efficiency could reach to 95% in 12 h in the pH range of 6–9. The effect of presence of some anions (Cl^- and NO_3^-) was negligible on the photocatalytic activity of MoS_2. It was predicted that hydroxyl radicals and holes played the role of reactive species in this process as indicated by scavengers' studies. The practicality of as-prepared MoS_2 photocatalyst was confirmed by using it in the removal of TBC from real water samples. Its stability and reusability were also ascertained in three successive runs.

Jiang et al.[15] fabricated hexagonal boron nitride (h-BN) decorated g-C_3N_4 metal-free heterojunction so that surface area is more and charge separation is also promoted. The photocatalytic activity of as-prepared h-BN/g-C_3N_4 composites was evaluated in

degradation of rhodamine B and tetracycline under visible light irradiation. It was observed that h-BN/g-C_3N_4 composites exhibited much higher photocatalytic activity as compared to g-C_3N_4 and h-BN. It was reported that photocatalytic efficiency of BC-3 sample was 2.3 and 60.3 times higher in degrading TC than its individual components g-C_3N_4 and h-BN, respectively. Similarly, it was also 7.3 and 11.8 times higher than g-C_3N_4 and h-BN for RhB degradation, respectively. This enhanced photocatalytic activity of h-BN/g-C_3N_4 composite was attributed to increase in surface area and h-BN nanosheet, which acted as promoter for photoexcited holes transfer.

Lu et al.[16] synthesized type II $ZnIn_2S_4/BiPO_4$ heterojunction via hydrothermal route. The morphology of as-prepared composite was dandelion-like microflower heterostructure. It was observed that the highest photocatalytic activity was there on using 70 wt% $ZnIn_2S_4/BiPO_4$ heterojunction, which can degrade about 84% tetracycline (40 mg L^{-1}) in 90 min. This activity was about 1.89 and 3.14 times higher as compared to $ZnIn_2S_4$ and $BiPO_4$, respectively. Improved separation efficiency of electron-hole pairs was mainly attributed due to type II heterojunction between $ZnIn_2S_4$ and $BiPO_4$, during the photocatalytic reaction. It was confirmed that •OH and $O_2^{\bullet -}$ were active oxidizing species in this photocatalytic system. Mahanthappa et al.[17]synthesized CuS, CdS and CuS-CdS nanocomposite photocatalysts via hydrothermal method. They also evaluated as-prepared materials for degradation of methylene blue in the presence of hydrogen peroxide (as an oxidant) under visible light irradiation. It was also revealed that about 80, 59 and 99.97% MB dye (10 ppm) degraded by could be degraded using for CuS, CdS and CuS-CdS nanocomposite, respectively in 10 min. This higher activity of CuS-CdS nanocomposite was attributed to narrow band gap, large surface area, low recombination of the photo-generated electrons and holes and high adsorbing capacity of the dye.

Tichapondwa et al.[18] examined the photocatalytic degradation of methylene blue using three commercially available TiO_2 powders with distinct crystalline phases as catalysts. The degradation experiments were performed on 10 ppm methylene blue solutions employing each of these powders. The results demonstrated that Degussa P25 TiO_2, which consists of a mixed phase of rutile and anatase, exhibited superior efficiency compared to pure anatase and rutile forms, showing a higher degradation capability 81.4% of the MB. About 95% degradation was achieved on using 0.5 g L^{-1} catalyst loading at pH 10. It was revealed that doping with copper increased degradation by 2% but zinc doping reduced it to 90%.

Kiwaan et al.[19] synthesized titanium dioxide photocatalyst via low temperature co-precipitation process and used for photocatalytic degradation of rhodamine B and acid red 57 (AR57) under UV irradiation. It was observed that the sample annealed at 400°C exhibited highest photocatalytic dye degradation efficiency of 93.8 and 90.7% for RhB and AR57, respectively in 190 min. It was found that degradation of RhB and AR57 involved $OH^{\bullet}$ radicals as main oxidizing species.

Tripathi et al.[20] described the synthesis of fluorescent selenium nanoparticles (SeNPs) utilizing Ficus benghalensis leaf extract. It was observed that the size distribution of these SeNPs was found to be in the range of 45–95 nm, and the average particle size was 64.03 nm. It was also revealed that as-synthesized SeNPs have been used for the photocatalytic degradation of methylene blue and 57.63% of dye degradation could be achieved in 40 min.

Aziz et al.[21] prepared chitosan-zinc sulfide nanoparticles (CS-ZnS-NPs). It was observed that their average particle size was 40 nm. The photocatalytic efficiency of as-prepared CS-ZnS-NPs was evaluated for degradation of acid brown 98 and acid black 234 using UV lamp (254 nm). It was reported that at optimal conditions, these NPs could degrade 96.7% acid black 234 in 100 min, while 92.6% for acid brown 98 was removed in 165 min. It was easily recovered and reused for four cycles.

Uheida et al.[22] developed a sustainable green photocatalytic technique for removal of microplastics from water using visible light. It was reported that photocatalytic degradation of microplastics, polypropylene (PP) (spherical particles) under visible light irradiation for two weeks of zinc oxide nanorods (ZnO NRs) (immobilized onto glass fibers) resulted in reduction of the average particle volume by 65%. The main photodegradation by-products were identified as mostly nontoxic in nature as evident from GC/MS analysis.

Liu et al.[23] synthesized $BiVO_4/Ag_3VO_4$ composite via a combination of hydrothermal and chemical deposition process. They subsequently applied the material for the degradation of methylene blue under visible light irradiation. The results indicated that the 40% $BiVO_4/Ag_3VO_4$ composite demonstrated superior photocatalytic performance, with a rate constant of 0.05588 min^{-1}. This value was approximately 1.76 and 22.76 times higher than those of Ag_3VO_4 (0.03167 min^{-1}) and $BiVO_4$ (0.00247 min^{-1}), respectively. Additionally, the composite exhibited good stability, retaining nearly 90% of its initial activity even after four successive cycles.

Badvi and Javanbakht prepared ZSM-5/TiO_2 nanophotocatalysts by dispersing TiO_2 onto the surface of ZSM-5 zeolite using a sol–gel method. The material was subsequently calcined at various temperatures and further modified with different loadings of nickel nanoparticles.

The photocatalytic activity of this material for methylene blue degradation was evaluated under UV light irradiation and compared with other treatment approaches, including catalytic hydrogen peroxide oxidation, hydrogen peroxide-assisted photocatalysis, and adsorption processes. The study reported that the highest degradation efficiency of 99.80% was achieved using 0.5% nickel nanoparticle loading at a calcination temperature of 600 °C.

Kumar et al. synthesized pristine copper–iron layered double hydroxide (LDH) doped with zirconium via a co-precipitation method, followed by incorporation with reduced graphene oxide. The resulting composite (ZrRGO–CuFe LDHs) was employed for the photodegradation of methylene blue in aqueous media. The incorporation of Zr and RGO enhanced the catalytic performance, yielding an effective heterogeneous catalyst with a band gap in the range of 1.74–2.0 eV.

The photocatalyst exhibited a high degradation efficiency of 95.2% within 75 minutes under visible light at pH 7, with a catalyst dosage of 1.0 g L^{-1} and methylene blue concentration of 10 ppm. Furthermore, approximately 92% of the total organic content was removed. The material also demonstrated good stability and reusability, maintaining performance over three consecutive cycles.

Peerakiatkhajohn et al. synthesized ZnO and aluminum-doped ZnO nanoparticles (Al/ZnO NPs) via a sol–gel method, employing different calcination temperatures (200, 300, and 400 °C) and varying aluminum concentrations (1, 3, 5, and 10%). It was observed that structure of ZnO NPs were spherical, nanorod and nanoflake for calcination temperatures at 200, 300 and 400° C, respectively. It was also revealed that ZnO NPs calcined at 200° C exhibited higher removal efficiency of methylene orange (80%) after 4 h under the UV light irradiation, due to more light absorption property and highest specific surface area, while 5% Al/ZnO samples displayed 99% removal efficiency in only 40 min, which was almost 20 times higher in photocatalytic activity as compared to pristine ZnO under visible light irradiation.

Qutub et al.[27] prepared cadmium sulphide nanostructures doped with titanium oxide (CdS/TiO_2) nanocomposites via a modified chemical precipitation method. The

photocatalytic performance of TiO_2/CdS nanocomposites was assessed under visible light irradiation. The results revealed that the synthesized CdS–TiO_2 nanocomposites achieved the highest photocatalytic efficiency, reaching 84% degradation of acid blue 29 (AB-29). In comparison, pure CdS and TiO_2 exhibited lower efficiencies of 68% and 9%, respectively, after 1 hour and 30 minutes of exposure to visible light. The enhanced activity of the CdS–TiO_2 system is primarily attributed to the suppression of charge carrier recombination and the improved visible-light responsiveness of TiO_2.

Almehizia et al.[28] prepared ZnO nanoparticles via combustion method using L-alanine, L-arginine and L-valine as organic fuels. It was reported that average crystallite size of these samples was 25.24, 31.11, and 35.65 nm on using L-arginine, L-valine, and L-alanine fuels, respectively. It was observed that these ZnO samples were of irregular, hexagonal, and spherical shapes respectively. The band gap of these ZnO samples was found to be 3.30, 2.88, and 2.63 eV, respectively. It was also revealed that these samples could degrade 50 mL of methylene blue (10 mg L^{-1}) dye under UV irradiations by 54.69, 41.34, and 30.76% in one and half h, respectively, however, it reached to 100% in presence of hydrogen peroxide within 70 min in case of L-arginine as fuel.

Verma et al.[29] developed titanium dioxide nanoparticles (TiO_2 NPs) along with titanium dioxide–graphene oxide (T/G) nanocomposites and applied both materials for the photocatalytic removal of methylene blue and malachite green dyes. Their findings indicated that approximately 85% of malachite green and 93% of methylene blue were degraded within 13 and 60 minutes, respectively, under visible light irradiation.

Wang et al.[30] fabricated a Z-scheme AgI/Sb_2WO_6 heterojunction using a chemical precipitation technique and employed it for the visible-light-driven degradation of rhodamine B and tetracycline. The study demonstrated degradation efficiencies of about 95% and 80% within 12 and 8 minutes, respectively, representing enhancements of 10.8 and 11.4 times compared to pure Sb_2WO_6.

Hwang et al.[31] synthesized a multifunctional photocatalyst by loading Co/Pd metal oxides onto acid-treated TiO_2 nanorods (ATO), followed by hydrogen incorporation through annealing. The hydrogen-treated catalyst (Pd(1)Co(1)/ATO (red)) showed remarkable degradation efficiencies of 99.63% for Orange II and 99.90% for bisphenol A (BPA) within 3 hours.

Pandeya et al.[32] produced flexible CdS/TiO_2 (CdS/TZ) nanofibrous membranes and evaluated their photocatalytic performance for methyl orange degradation. The composite membrane achieved a degradation efficiency of 96.8% within 1 hour and maintained its activity over five successive cycles. Additionally, the chemical oxygen demand (COD) removal efficiency increased from 74.16% for pure TiO_2 membranes to 91.66% for the CdS/TiO_2 composite.

Masekela et al.[33] immobilized a tri-component Sb–ZnO/MoS_2 system onto fluorine-doped tin oxide (FTO) substrates and investigated its catalytic performance for degrading methyl orange, methylene blue, and ciprofloxacin under combined light and ultrasonic irradiation. The synergistic effect of photocatalysis and piezocatalysis resulted in degradation efficiencies of 95%, 82%, and 72% for methylene blue, methyl orange, and ciprofloxacin, respectively. Furthermore, total organic carbon (TOC) analysis revealed mineralization degrees of 76%, 70%, and 52% for MB, MO, and CIP, respectively.

Qing et al.[34] prepared composite membranes incorporating polyvinylidene fluoride (PVDF)

as the base material, polyvinylpyrrolidone (PVP) as a dispersing and wettability-enhancing agent, and cuprous oxide as the active photocatalyst. These membranes were subsequently utilized for the photocatalytic degradation of methyl orange, methylene blue, and Congo red dyes. It was also revealed that higher photocatalytic degradation ratio for methyl orange (93.6%) was there. This as-prepared membrane also had excellent recycling stability, and it can retain its removal ability to 92.1% even after using it 5 times. It was reported that these composite membranes also displayed high removal ability of methylene blue (81.4) and (76.1%).

Advanced oxidation processes (AOPs) are emerging as a potential technology for the treatment of pollutant water. Out of these, photocatalysis plays a dominant role to degrade organic contaminants to almost harmless or less harmful products. It is also a green chemical pathway as it takes care of environment in advance[36-40].

Conclusion

Advances in photocatalytic catalysts have significantly transformed wastewater treatment by enabling efficient, sustainable, and low-energy degradation of a wide range of organic and inorganic pollutants. The evolution from conventional semiconductor systems such as titanium dioxide to advanced nanostructured and hybrid materials—including doped catalysts, heterojunction systems, and carbon-based nanomaterials—has markedly improved light absorption, charge separation efficiency, and overall catalytic performance. These innovations have expanded photocatalytic activity into the visible-light spectrum, making solar-driven treatment increasingly viable.

Furthermore, the integration of emerging materials such as graphene oxide, metal–organic frameworks, and plasmonic nanoparticles has enhanced pollutant selectivity and reaction kinetics. Coupling photocatalysis with complementary technologies, such as membrane filtration and biological treatments, has also demonstrated synergistic effects, leading to higher degradation efficiencies and mineralization rates.

Despite these advancements, several challenges remain, including catalyst stability, large-scale implementation, recovery and reusability of nanocatalysts, and cost-effectiveness. Future research should focus on designing robust, scalable, and environmentally benign photocatalysts, alongside reactor engineering and process optimization for real-world applications.

Overall, photocatalytic wastewater treatment represents a promising frontier in environmental remediation, aligning with global sustainability goals by offering green, efficient, and versatile solutions for water purification.

References:

1. Ledakowicz, S., Solecka, M., and Zylla, R., Biodegradation, decolourisation and detoxification of textile wastewater enhanced by advanced oxidation processes, *J. Biotechnol.*,**2001**, 89(2-3), 175-184.
2. Tang, J., Zou, Z., Yin, J., and Ye, J., Photocatalytic degradation of methylene blue on $CaIn_2O_4$under visible light irradiation, *Chem. Phys. Lett.*, **2003**, 382(1-2), 175-179
3. Liqiang, J., Baiqi, W., Baifu, X., Shudan, L., Keying, S., Weimin, C., et al., Investigations on the surface modification of ZnO nanoparticle photocatalyst by depositing Pd, *J. Solid State Chem.*,**2004,** 177(11), 4221-4227.
4. Chen, F., Zou, W., Qu, W., and Zhang, J., Photocatalytic performance of a visible light TiO_2 photocatalyst prepared by a surface chemical modification process, *Catal.*

Commun., **2009,** 10(11), 1510-1513.
5. Wu, Y., Xing, M., Zhang, J., and Chen, F., Effective visible light-active boron and carbon modified TiO_2 photocatalyst for degradation of organic pollutant, *Appl. Catal. B: Environ.*, **2010,** 97(1-2), 182-189.
6. Pan, C., and Zhu, Y., New type of $BiPO_4$ oxy-acid salt photocatalyst with high photocatalytic activity on degradation of dye, *Environ. Sci. Technol.*,**2010,** 44(14), 5570-5574.
7. Yu, H., Xu, L., Wang, P., Wang, X., and Yu, J., Enhanced photoinduced stability and photocatalytic activity of AgBr photocatalyst by surface modification of Fe (III) cocatalyst, *Appl. Catal. B: Environ.*, **2014,**144, 75-82.
8. Bai, X., Wang, L., Wang, Y., Yao, W., and Zhu, Y., Enhanced oxidation ability of g-C_3N_4 photocatalyst via C_{60} modification, *Appl. Catal. B: Environ.*, **2014,** 152, 262-270.
9. Tripathy, N., Ahmad, R., Song, J. E., Ko, H. A., Hahn, Y. B., and Khang, G., Photocatalytic degradation of methyl orange dye by ZnO nanoneedle under UV irradiation, *Mater. Lett.*, **2014,**136, 171-174.
10. Balcha, A., Yadav, O. P., and Dey, T., Photocatalytic degradation of methylene blue dye by zinc oxide nanoparticles obtained from precipitation and sol-gel methods, *Environ. Sci. Pollut. Res.*, **2016,** 23, 25485-25493. doi.org/10.1007/ s11356-016-7750-6.
11. Thi, V. H. T., and Lee, B. K., Effective photocatalytic degradation of paracetamol using La-doped ZnO photocatalyst under visible light irradiation, *Mater. Res. Bull.*, **2017,** 96, 171-182.
12. Sudrajat, H., and Babel, S., A novel visible light active N-doped ZnO for photocatalytic degradation of dyes, *J. Water Process. Eng.*, **2017,** 16, 309-318.
13. Wu, Y., Wang, H., Tu, W., Liu, Y., Tan, Y. Z., Yuan, X., et al., Quasi-polymeric construction of stable perovskite-type $LaFeO_3$/g-C_3N_4 heterostructured photocatalyst for improved Z-scheme photocatalytic activity via solid pn heterojunction interfacial effect, *J. Hazard. Mater.*, **2018,** 347, 412-422.
14. Huang, S., Chen, C., Tsai, H., Shaya, J., and Lu, C., Photocatalytic degradation of thiobencarb by a visible light-driven MoS_2 photocatalyst, *Sep. Purif. Technol.*, **2018,** 197, 147-155.
15. Jiang, L., Yuan, X., Zeng, G., Wu, Z., Liang, J., Chen, X., et al., Metal-free efficient photocatalyst for stable visible-light photocatalytic degradation of refractory pollutant, *Appl. Catal. B: Environ.*, **2018,** 221, 715-725.
16. Lu, C., Guo, F., Yan, Q., Zhang, Z., Li, D., Wang, L., et al., Hydrothermal synthesis of type II $ZnIn_2S_4$/$BiPO_4$ heterojunction photocatalyst with dandelion-like microflower

structure for enhanced photocatalytic degradation of tetracycline under simulated solar light, *J. Alloys Compd.*, **2019,** 811, doi.org/10.1016/ j.jallcom.2019.151976.
17. Mahanthappa, M., Kottam, N., and Yellappa, S., Enhanced photocatalytic degradation of methylene blue dye using CuSCdS nanocomposite under visible light irradiation, *Appl. Surf. Sci.*, **2019,** 475, 828-838. doi.org/10.1016/ j. apsusc.2018.12.178.
18. Tichapondwa, S. M., Newman, J. P., and Kubheka, O., Effect of TiO_2 phase on the photocatalytic degradation of methylene blue dye, *Phys. Chem. Earth., Parts A/B/C*, **2020,** 118, doi.org/10.1016/j.pce.2020.102900.
19. Kiwaan, H. A., Atwee, T. M., Azab, E. A., and El-Bindary, A. A., Photocatalytic degradation of organic dyes in the presence of nanostructured titanium dioxide, *J. Mol. Struct.*, **2020,** 1200, doi.org/10.1016/j.molstruc.2019.127115.
20. Tripathi, R. M., Hameed, P., Rao, R. P., Shrivastava, N., Mittal, J., and Mohapatra, S., Biosynthesis of highly stable fluorescent selenium nanoparticles and the evaluation of their photocatalytic degradation of dye, *Bionanosci.*, **2020,**10, 389-396.
21. Aziz, A., Ali, N., Khan, A., Bilal, M., Malik, S., Ali, N., and Khan, H., Chitosan-zinc sulfide nanoparticles, characterization and their photocatalytic degradation efficiency for azo dyes, *Int. J. Biol. Macromol.*, **2020,** 153, 502-512. doi.org/10.1016/j.ijbiomac.2020.02.310
22. Uheida, A., Mejía, H. G., Abdel-Rehim, M., Hamd, W., and Dutta, J., Visible light photocatalytic degradation of polypropylene microplastics in a continuous water flow system, *J. Hazard. Mater.*, **2021,** 406, doi.org/10.1016/j.jhazmat.2020.124299.
23. Liu, L., Hu, T., Dai, K., Zhang, J., and Liang, C., A novel step-scheme $BiVO_4/Ag_3VO_4$ photocatalyst for enhanced photocatalytic degradation activity under visible light irradiation, *Chinese J. Catal.*, **2021,** 42(1), 46-55.
24. Badvi, K., and Javanbakht, V., Enhanced photocatalytic degradation of dye contaminants with TiO_2 immobilized on ZSM-5 zeolite modified with nickel nanoparticles, *J. Clean. Prod.*, **2021,** 280, doi.org/10.1016/j.jclepro.2020.124518.
25. Kumar, O. P., Ashiq, M. N., Shah, S. S. A., Akhtar, S., Obaidi, M. A. A., Mujtaba, et al., Nanoscale ZrRGOCuFe layered double hydroxide composites for enhanced photocatalytic degradation of dye contaminant, *Mater. Sci. Semicond. Process.*, **2021,** 128, doi.org/10.1016/j.mssp.2021.105748.
26. Peerakiatkhajohn, P., Butburee, T., Sul, J. H., Thaweesak, S., and Yun, J. H., Efficient and rapid photocatalytic degradation of methyl orange dye using Al/ZnO nanoparticles, *Nanomater.,* **2021,** 11(4), doi.org/10.3390/nano11041059.
27. Qutub, N., Singh, P., Sabir, S., Sagadevan, S., and Oh, W. C., Enhanced photocatalytic degradation of acid blue dye using CdS/TiO_2 nanocomposite, *Sci. Rep.*, **2022,** 12(1), doi: 10.1038/s41598-022-09479-0.
28. Almehizia, A. A., Al-Omar, M. A., Naglah, A. M., Bhat, M. A., and Al-Shakliah, N. S., Facile synthesis and characterization of ZnO nanoparticles for studying their biological activities and photocatalytic degradation properties toward methylene blue dye, *Alex. Eng. J.*, **2022,** 61(3), 2386-2395. doi.org/10.1016/j.aej.2021.06.102.
29. Verma, N., Chundawat, T. S., Chandra, H., and Vaya, D., An efficient time reductive photocatalytic degradation of carcinogenic dyes by TiO_2-GO nanocomposite, *Mater. Res. Bull.*, **2023, *158*,** doi.org/10.1016/j.materresbull. 2022.112043.
30. Z. Wang, W. Li, J. Wang, Y. Li, G. Zhang, Novel Z-scheme $AgI/Sb_2 WO_6$ heterostructure for efficient photocatalytic degradation of organic pollutants under

visible light: Interfacial electron transfer pathway, DFT calculation and mechanism unveiling, *Chemosphere*, **311**, **2023**
doi.org/10.1016/j.chemosphere.2022.137000
31. I. S. Hwang, V. Manikandan, R. P. Patil, M. A. Mahadik, W.-S. Chae, H.-S. Chung, S. H. Choi, and J. S. Jang, Hydrogen-treated TiO_2 nanorods decorated with bimetallic Pd–Co nanoparticles for photocatalytic degradation of organic pollutants and bacterial inactivation, *ACS Appl. Nano Mater*. **2023 6** (3), 1562-1572
32. doi: 10.1021/acsanm.2c04160
33. S. Pandeya, R. Ding, Y. Ma, X. Han, M. Gui, P. Mulmi, K. P. Panthi, B. B. Neupane, H. R. Pant, Z. Li, M. K. Joshi, Self-standing CdS/TiO_2 Janus nanofiberous membrane: COD removal, antibacterial activity and photocatalytic degradation of organic pollutants, *J. Environ. Chem. Eng.,* **12**(3), **2024** doi.org/10.1016/j.jece.2024.112521
34. D. Masekela, N. C. Hintsho-Mbita, L. N. Dlamini, T. L. Yusuf, N. Mabuba, Internal piezoelectric field produced by tri-component (FTO: Sb-ZnO/MoS_2) thin film for enhanced photocatalytic degradation of organic pollutants and antibacterial activity, *Mater. Today Commun*., **38**, **2024** doi.org/10.1016/j.mtcomm.2024.108500
35. Q. Qing, S.-Y. Chen, S.-Z. Hu, L. Li, T. Huang, N. Zhang, and Y. Wang, highly efficient photocatalytic degradation of organic pollutants using a polyvinylidene fluoride/polyvinylpyrrolidone-cuprous oxide composite membrane, *Langmuir* **2024 40** (2), 1447-1460, doi: 10.1021/acs.langmuir.3c03168
36. S.Ravichandran, Synth.Commun., 31(13), 2055-2057,2001.
37. N.Raman and S.Ravichandran. Asian J. Chem., 15(3&4), 1848-1850, 2003.
38. N.Raman and S.Ravichandran. Polish J. Chem., 78,2005-2012, 2004.
39. Kudo, A.; Miseki, Y. *Chem. Soc. Rev.*, *38*, 253–278(2009).
40. K.P.Satheesh,S.Ravichandran and K.B.Chandrasekar ,Int.J.Chem.Tech.Res., 3(4), 1740-1746, 2011.